J Physiol 589.12 (2011) pp 2927–2934

SYMPOSIUM REVIEW

Lymphatic anatomy and biomechanics

Daniela Negrini and Andrea Moriondo

Department of Experimental and Clinical Biomedical Sciences, University of Insubria, 21100 Varese, Italy

Abstract Lymph formation is driven by hydraulic pressure gradients developing between the interstitial tissue and the lumen of initial lymphatics. While in vessels equipped with lymphatic smooth muscle cells these gradients are determined by well-synchronized spontaneous contractions of vessel segments, initial lymphatics devoid of smooth muscles rely on tissue motion to form lymph and propel it along the network. Lymphatics supplying highly moving tissues, such as skeletal muscle, diaphragm or thoracic tissues, undergo cyclic compression and expansion of their lumen imposed by local stresses arising in the tissue as a consequence of cardiac and respiratory activities. Active muscle contraction and not passive tissue displacement is required to support an efficient lymphatic drainage, as suggested by the fact that the respiratory activity promotes lymph formation during spontaneous, but not mechanical ventilation. The mechanical properties of the lymphatic wall and of the surrounding tissue also play an important role in lymphatic function. Modelling of stress distribution in the lymphatic wall suggests that compliant vessels behave as reservoirs accommodating absorbed interstitial fluid, while lymphatics with stiffer walls, taking advantage of a more efficient transmission of tissue stresses to the lymphatic lumen, propel fluid through the lumen of the lymphatic circuit.

(Received 1 February 2011; accepted after revision 7 April 2011; first published online 11 April 2011)
Corresponding author D. Negrini: Dipartimento di Scienze Biomediche Sperimentali e Cliniche, Università degli Studi dell'Insubria, Via J.H. Dunant 5, 21100 Varese, Italy. Email: daniela.negrini@uninsubria.it

Vascular and extravascular fluid compartments forces cause a net filtration of fluid and solutes from the microvasculature to the surrounding interstitium. Hypovolaemia and development of tissue oedema is prevented, in most organs, by the lymphatic system that, in normal conditions, efficiently removes excess interstitial fluid, solutes and cells and returns them to the bloodstream, thus maintaining normal plasma and interstitial fluid volume and solute concentration.

The lymphatic system is a closed network originating from the interstitial tissue with the *initial lymphatics*, small capillaries delimited by a discontinuous endothelium and basement membrane offering low resistance to the passage of fluid, hydrophilic molecules of any size, cells, viruses

Daniela Negrini has a degree in Biological Sciences from the University of Milan. She has a broad interest in the mechanisms controlling tissue fluid homeostasis, in particular on the lymphatic drainage of lung parenchyma and thoracic tissues. At the University of Insubria, she is currently investigating the role of the extracellular matrix in modulating the lymphatic function under normal and pathophysiological conditions. **Andrea Moriondo** has a degree in Biological Sciences and a PhD in Neurobiology and Neurophysiology from the University of Milan. His research interests include the mechanical and electrophysiological properties of endothelial and smooth muscle cells in initial lymphatics.

This report was presented at *The Journal of Physiology* Symposium on *Physiology, pharmacology and pathology of tissue fluid exchange*, which took place at the 31st International Symposium on Intensive Care and Emergency Medicine, Brussels, Belgium on 22 March 2011. It was commissioned by the Editorial Board and reflects the views of the author.

DOI: 10.1113/jphysiol.2011.206672

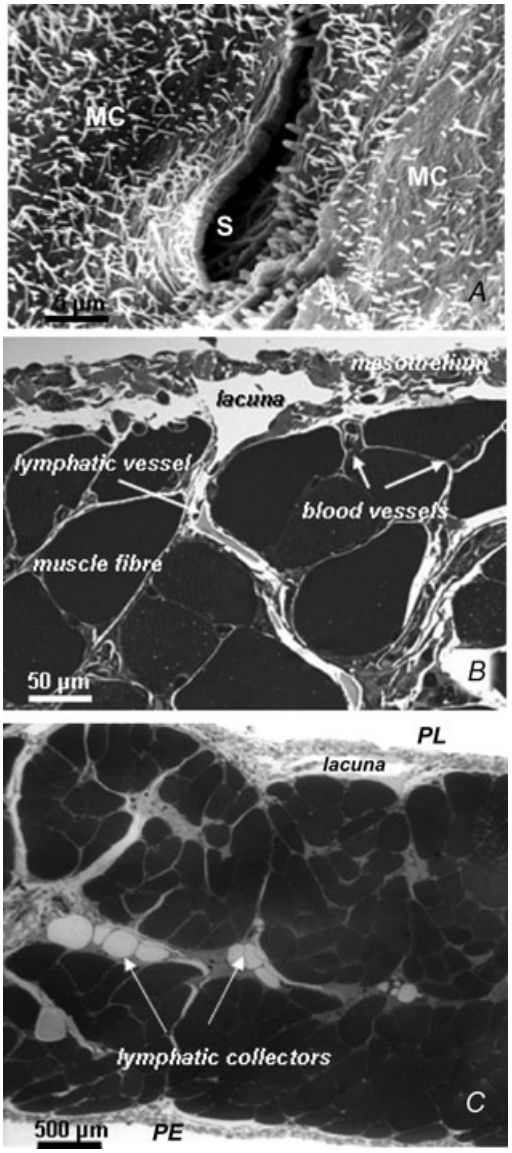

Figure 1. Arrangement of the diaphragmatic lymphatic network
A, scanning electron photomicrograph of an elliptical lymphatic stoma on the tendinous pleural surface of the rat diaphragm. The stoma (S), delimited by a net border, opens at the confluence between adjacent mesothelial cells (MC) characterized by a mesh of microvilli protruding from the cell surface. *B*, semi-thin cross-section of rat pleural hemi-diaphragm stained with crystal violet and basic fuchsin showing the arrangement of the diaphragmatic lymphatic network originating from the pleural mesothelial surface. Lymphatic submesothelial lacunae located within the interstitial space beneath the mesothelial layer are in continuity with transverse lymphatic vessels (arrow) located in the deep interstitial space and running perpendicularly to the lacunae and through the diaphragmatic skeletal muscular fibres. *C*, semi-thin cross-section of rat entire diaphragm stained with crystal violet and basic fuchsin, showing both the pleural (PL) and the peritoneal (PE) mesothelial surfaces. Transverse lymphatic vessels departing from the pleural and peritoneal submesothelial lacunae empty into central lymphatic collectors, located in the deep interstitial space, which receive the lymph collected from both surfaces of the diaphragm.

and bacteria from the interstitial space into the lymphatic lumen (Schmid-Schöenbein, 1990). Anchoring filaments of collagen VII (Sakai *et al.* 1986; Keene *et al.* 1987) connect the outer endothelial cell surface to matrix fibres (Burgeson *et al.* 1990; Chen *et al.* 1997; Rousselle *et al.* 1997), and allow mechanical transmission of tissue forces to the lymphatic lumen. Lymphatic capillaries are devoid of smooth muscle cells; however, actin-like filaments have been observed within the endothelial cells (Casley-Smith & Florey, 1961; Leak, 1970; Tsilibary & Wissig, 1983; Castenholz, 1987). Initial lymphatics merge into larger *collecting lymphatics or collecting ducts* (diameter $> 200\,\mu$m), characterized by a stratified wall equipped with smooth muscle cells arranged in the media externally to the endothelial cell layer and interspersed with collagen and elastic fibres (Ohhashi *et al.* 1980; Reddy & Staub, 1981).

In spite of the recognized importance of tissue motion on lymph function, details of the mechanism through which the tissue matrix contributes to lymph formation and progression in initial lymphatics have not been completely elucidated yet, due to difficulties encountered in approaching the initial lymphatics *'in vivo'*. A favourable experimental model to study this issue is the lymphatic network supplying the parietal pleura lining the thoracic wall, the intercostal muscles, the mediastinum and the diaphragm (Miserocchi *et al.* 1982, 1989; Negrini *et al.* 1991, 1992). The pleural lymphatic circuit departs from the pleural space through the 'stomata' (Fig. 1*A*), discontinuities of the mesothelium formed at the confluence between mesothelial cells (Wang, 1975, 1998; Negrini *et al.* 1991). The conduit network is hierarchically organized in (a) submesothelial lacunae (Fig. 1*B*), which receive the pleural fluid drained through the stomata (Negrini *et al.* 1992; Grimaldi *et al.* 2006), (b) transverse vessels, departing from the submesothelial lacunae and running through the skeletal muscle fibres (Fig. 1*C*), and (c) deeper lymphatic collectors (Fig. 1*B* and *C*), which eventually convey the lymph outside the diaphragm (Grimaldi *et al.* 2006). The endothelium of the initial lymphatic lies in close proximity to extracellular matrix fibres and skeletal muscle cells (Fig. 2*A* and *B*) and is characterized by the presence of two types of unidirectional valves. *Primary valves* (Fig. 3*A*) are formed by cytoplasmic extension of adjacent endothelial cells linked by tight junctions (Trzewik *et al.* 2001; Grimaldi *et al.* 2006); they protrude into the lumen, forming a funnel-like, unidirectional entrance which regulates fluid entrance into the lumen (Galie & Spilker, 2009) and prevents fluid back-flow. *Intraluminar valves* (Fig. 3*B*) consist of two endothelial leaflets attached at opposite sites to the lymph channel and connected with zonulae (Takada, 1971); they are regularly spaced along the network, from small initial lymphatics to large collecting ducts. The segment delimited by two consecutive intraluminar valves,

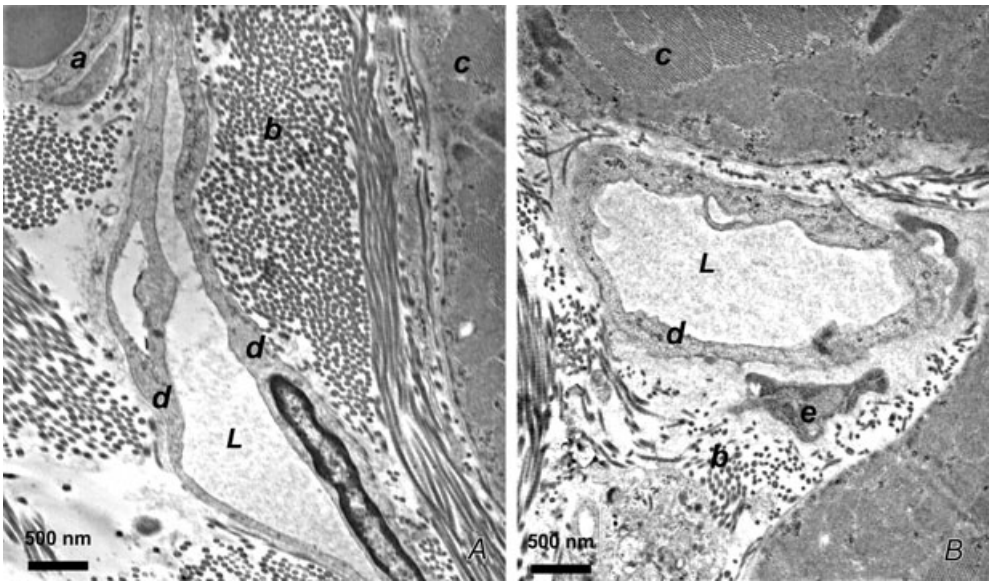

Figure 2. Anatomical proximity of initial lymphatic lumen and interstitial fibrillar structures
A and *B*, transmission electron microphotographs of thin sections of rat diaphragm. Initial lymphatics run through connective tissue composed of loose collagen fibres organized in bundles (b) adjacent to the skeletal muscular fibres (c). These vessels are characterized by typical ultrastructural features: absence of smooth muscle fibres, thin endothelial wall, discontinuous basal lamina, tight junctions or overlapping contacts and anchoring filaments linking the endothelial cells to the adjacent collagen fibres and to muscle fibre sarcolemma. L, lymphatic lumen; a, vascular capillary endothelium; b, collagen bundles; c, skeletal muscle fibres; d, lymphatic endothelium; e, fibroblast.

or 'lymphangion', is considered the 'functional unit' of the lymphatic vascular system.

In initial lymphatics, lymph flow (J_{lymph}) through the interendothelial junctions can be described (Granger *et al.* 1984) as:

$$J_{\text{lymph}} = K_{\text{lymph}}(P_{\text{int}} - P_{\text{lymph}}) = K_{\text{lymph}} \times \Delta P_{\text{TM}} \quad (1)$$

where K_{lymph} is lymphatic conductance, P_{int} and P_{lymph} are the interstitial and lymphatic fluid pressure and ΔP_{TM} the transmural pressure gradient acting across the lymphatic wall, respectively. Equation 1 implies that lymphatic permeability is constant, a simplified assumption that might be reconsidered in light of the evidence of an outwardly directed and convectively coupled albumin flux in mesenteric collecting lymphatics (Scallan & Huxley, 2010). This finding, contradicting the common belief that lymphatics can only support absorption (Aukland & Reed, 1993), also clearly indicates that further studies on the regulation of initial and collecting vessel lymphatic wall permeability, on the modulatory mechanisms and

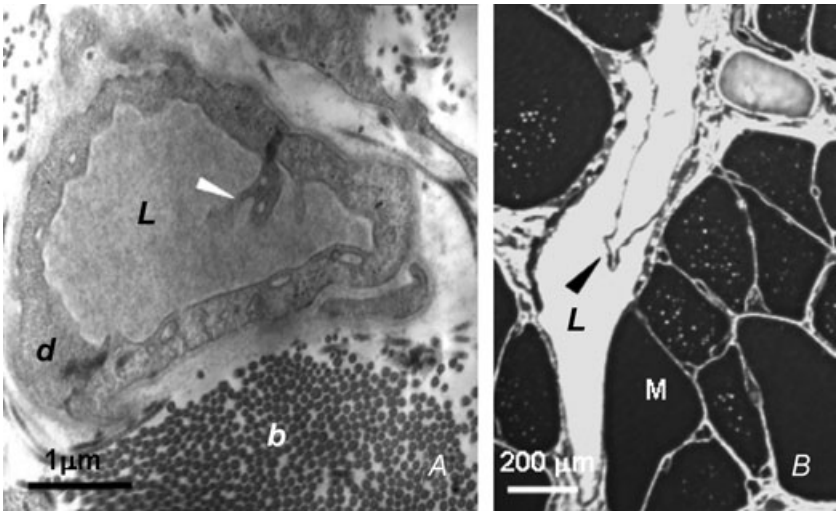

Figure 3. Lymphatic unidirectional valves
A, transmission electron microphotographs showing the primary unidirectional valves (white arrowhead) in the wall of diaphragmatic initial lymphatics located in the pleural submesothelial interstitium. The valves are formed at the junction between overlapping cytoplasmic extensions of two adjacent lymphatic endothelial cells (d) (reproduced from Grimaldi *et al.* 2006). *B*, semi-thin sections of transverse lymphatic ducts, showing a unidirectional intraluminar, or secondary, valve formed by two leaflets (arrowhead) attached at opposite sides of the lymph channel wall. L, lymphatic lumen; b, collagen bundles; M, skeletal muscle fibres; d, lymphatic endothelium (reproduced from Grimaldi *et al.* 2006).

on the variability of the lymphatic networks supplying different organs are needed to elucidate the complexity of the lymphatic function.

J_{lymph} directly depends upon P_{int}, which in turn reflects: (a) changes in local tissue stress elicited by tissue movements and/or (b) increased interstitial fluid volume. In vessels equipped with lymphatic smooth muscle cells, ΔP_{TM} is supported by spontaneous contractions of the lymphangion wall (Mawhinney & Roddie, 1973; Zweifach & Prather, 1975; McHale & Roddie, 1976; Hargens & Zweifach, 1977; Ohhashi *et al.* 1980; Benoit *et al.* 1989). In initial lymphatics devoid of smooth muscles, ΔP_{TM} is instead sustained, during normal tissue hydration, by cyclic compression and expansion of the lymphatic lumen caused by local external tissue movements (Schmid-Schöenbein, 1990; Aukland & Reed, 1993), such as those encountered in thoracic tissues in relation to the cardiac and respiratory activity. Cardiogenic oscillations of diaphragmatic P_{int} and P_{lymph} (Fig. 4*A*), for example, depend upon: (a) small displacements of lung parenchyma, pleural fluid and diaphragm accompanying systolic/diastolic myocardial volume changes, and (b) transmission of arterial pressure waves along the walls of large thoracic arteries. Respiratory-induced P_{int} and P_{lymph} changes have been recorded (Fig. 4*B*) in intercostal tissue and lymphatics during spontaneous inspiration (Moriondo *et al.* 2005), a mechanically complex situation causing lung expansion through: (a) contraction and shortening of external intercostal and diaphragmatic muscular fibres; (b) ribs and diaphragm displacement and increased chest volume; (c) decreased pleural liquid pressure. The average ΔP_{TM} (eqn (1)) developing across the initial lymphatic wall as a result of cardiogenic or respiratory P_{int} and P_{lymph} swings amounts to 4–10 mmHg, indicating the capability of tissue motion to sustain, *per se*, local lymph formation in the thoracic tissues (Negrini & Del Fabbro, 1999; Negrini *et al.* 2004; Moriondo *et al.* 2005). In addition to their direct mechanical role, tissue matrix macromolecules might modulate local lymphatic function through active matrix-related signalling pathways, similar to observations in vascular wall cells (Davis *et al.* 2001; Hocking *et al.* 2008; Sun *et al.* 2008; Stratman *et al.* 2009; Rutkowski *et al.* 2010). Interestingly, when neuromuscular transmission is blocked in rats and they are mechanically ventilated at zero end-expiratory alveolar pressure, average ΔP_{TM} is essentially nullified, indicating that active intercostal muscle contraction and not the change in chest wall volume is required to support lymphatic function (Fig. 4*C*).

For tissue displacements to generate pressure gradients promoting lymph production and progression, local tissue stresses must be transmitted to the lymphatic vessel lumen and converted into intraluminar pressure waves. In turn, force transmission is influenced by the mechanical properties of the vessel wall, being more effective in stiff compared to distensible structures. The mechanical behaviour of diaphragmatic submesothelial lymphatics, treated as cylindrical tubes with elastic walls, was analysed by measuring the wall compliance, C_{lymph}, in conditions as close as possible to the physiological state (Moriondo *et al.* 2010). The experiments delivered multiple sequential

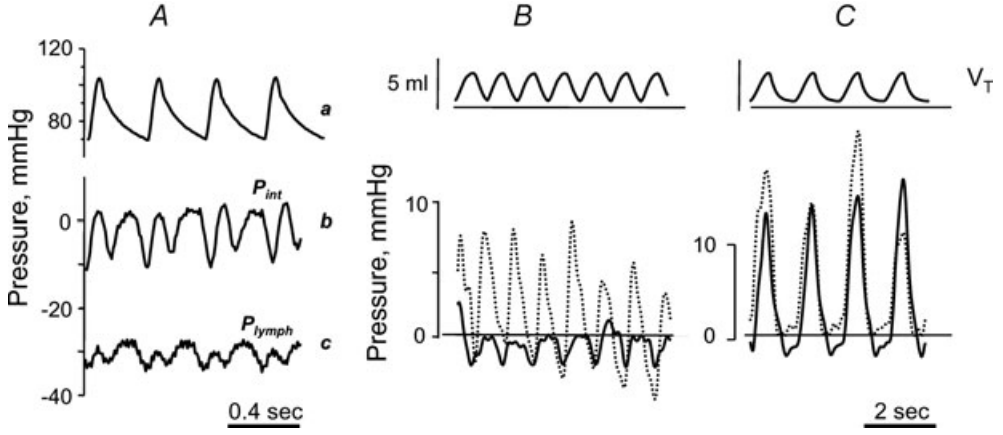

Figure 4. Effect of cardiac and respiratory activity on interstitial (P_{int}) and lymphatic (P_{lymph}) fluid pressure
A, cardiogenic oscillations of diaphragmatic interstitial (*b*, P_{int}) and intraluminar lymphatic pressure (*c*, P_{lymph}), measured through the micropuncture technique in anaesthetized rats under neuromuscular blockade. Both diaphragmatic P_{int} and P_{lymph} oscillate almost in phase with arterial systemic pressure (*a*), shifting from a minimum to a maximum value during cardiogenic oscillations (modified from Negrini *et al.* 2004). *B* and *C*, simultaneous recording of respiratory tidal volume (V_T, top panel), lymphatic (P_{lymph}; continuous lines) and interstitial (P_{int}; dashed lines) pressures obtained in intercostal lymphatics of supine anaesthetized rats during spontaneous breathing (*B*) or mechanical ventilation at similar V_T and at zero alveolar end-expiratory pressure (*C*) (modified from Moriondo *et al.* 2005).

injections of 4.6 nl of lissamine green-coloured saline solution into a lymphatic segment lumen through an injecting micropipette, while simultaneously recording P_{lymph} with another micropipette inserted in the same vessel. As shown in the example of Fig. 5*A*, each injection caused a sharp increase ($\Delta P_{lymph-peak}$) of baseline P_{lymph} to a transient peak pressure ($P_{lymph-peak}$), followed by a slow decay toward the pre-injection value. C_{lymph} was calculated as the slope of the relationship obtained by plotting the cumulative injected volume ($V_{injected}$) as a function of the corresponding $P_{lymph-peak}$ (Fig. 5*B*). The results revealed the existence of a population of distensible, highly compliant vessels (high-C_{lymph}, H-$C_{lymph} = 6.7 \pm 1.6$ nl mmHg^{-1}) and, within the same submesothelial circuit, of another population of significantly stiffer (low-C_{lymph}, L-$C_{lymph} = 1.5 \pm 0.4$ nl mmHg^{-1}) lymphatics. The investigated vessels' size and alignment with respect to the underlying muscular fibres were relatively uniform, so that observed H-C_{lymph} and L-C_{lymph} differences could not be ascribed to vessel geometry. The C_{lymph} variability might otherwise depend upon (a) the stiffness of the mesothelium and of the diaphragmatic muscular or tendinous tissue, and (b) the relative percentage of compliant or stiff tissue in the vessel wall. Indeed, the endothelium of the most superficial diaphragmatic lymphatics is delimited almost entirely by the mesothelium (Fig. 1*A* and *B*), while deeper vessels within the same submesothelial circuit are surrounded by the muscular and tendinous tissue over most of their surface (Grimaldi *et al.* 2006).

The mechanical behaviour of the diaphragmatic tissue was assessed by evaluating the elastic modulus of the tissue (E_t) at various strain levels. In excised preconditioned diaphragmatic tissue strips exposed to standard stress relaxation tests, the force applied to the strip and tissue displacements were recorded and then processed to obtain strains (ε) and stresses (σ). The step-wise test consisted of four strain ramps, each 5% of the sample initial length, at a velocity of 10% s^{-1}, followed by stress relaxation to equilibrium. E_t was then calculated as:

$$E_t = \frac{\Delta\sigma}{\Delta\varepsilon} \qquad (2)$$

where $\Delta\sigma$ and $\Delta\varepsilon$ are the change of equilibrium stress (i.e. at the end of stress relaxation) and variation of strain between successive ramps, respectively.

On the assumption that lymphatics and diaphragmatic tissue behave as linear isotropic materials, a finite element model was applied to describe the mechanical response of three diaphragmatic lymphatics distinguished on the basis of different composition of their wall: (a) a superficial one, laying over the muscular/tendinous diaphragmatic plane, delimited almost entirely by the mesothelium (Fig. 6*A*); (b) an 'intermediate' one, surrounded partly by the mesothelium, and partly by stiffer muscular/tendinous tissue (Fig. 6*B*), and (c) a deep one, completely immersed in stiff tissue (Fig. 6*C*). Tissue stiffness was expressed by its elastic modulus before failure ($E_{t,f}$), and C_{lymph} was calculated from the model ($C_{lymph-M}$) as:

$$C_{lymph-M} = \frac{\Delta V}{\Delta P_{TM}} = \frac{\pi r_{min} \times r_{max} \times l}{\Delta P_{TM}} \qquad (3)$$

where ΔV is the lymphatic volume change for a given ΔP_{TM}, r_{min} and r_{max} are the smaller and greater average vessel radii and l the vessel length for an average ΔP_{TM} of 10 mmHg. The modelling suggests that the proportion of stiff tissue in the lymphatic vessel wall does determine its mechanical properties. Indeed, the C_{lymph} (0.07 nl mmHg^{-1}) of deep vessels surrounded by

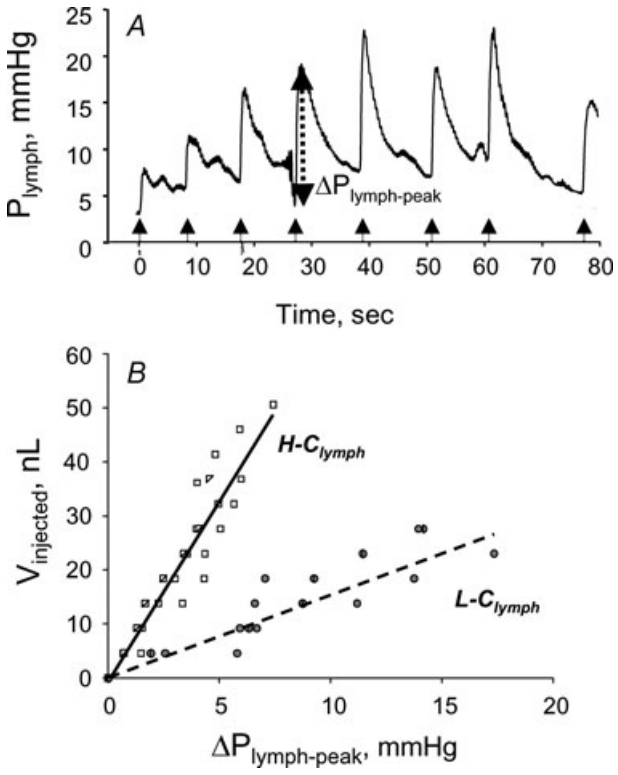

Figure 5. Pressure–volume behaviour of submesothelial diaphragmatic lymphatics
A, time course of P_{lymph} from the pre-injection value at $t = 0$ and during sequential injections of 4.6 nl of lissamine green saline solution. At each injection P_{lymph} sharply increases by $\Delta P_{lymph-peak}$ to attain a peak value followed by a slower P_{lymph} decay to pre-injection values (modified from Moriondo *et al.* 2010). *B*, relationships obtained by pooling data from several measurements in different diaphragmatic submesothelial vessels, where the cumulative injected volume, $V_{injected}$, is plotted as a function of $\Delta P_{lymph-peak}$. The data points appear distributed in two distinct populations characterized by a significantly ($P < 0.05$) different C_{lymph} amounting to 6.7 nl mmHg^{-1} (high compliance, H-C_{lymph}) and 1.5 nl mmHg^{-1} (low compliance, L-C_{lymph}), respectively (modified from Moriondo *et al.* 2010).

stiff tissue (Fig. 6*C*) is up to ∼2 orders of magnitude lower compared to submesothelial vessels mostly or partly surrounded by compliant mesothelium (Fig. 6*A* and *B*). In relaxed isolated mesenteric lymphatics C_{lymph} is intermediate (Zhang *et al.* 2007) between those measured in submesothelial and deep diaphragmatic vessels, suggesting that the smooth muscle cell layer may not only sustain active lymphatic pumping, but also provide a relatively stiff mechanical support to lymphatic networks supplying soft tissues.

Wall stiffness also influences the distribution of circumferential stresses in the vessel wall, represented in Fig. 6 by colour shade and intensity. For a given ΔP_{TM}, higher tensile stresses develop in the compliant wall of superficial (Fig. 6*A*) and of intermediate lymphatics (Fig. 6*B*) at the edges between the compliant mesothelium and the stiff tissue basement. Lower wall tension, more homogeneously distributed over the entire surface, develops in deeper, stiffer lymphatics (Fig. 6*C*).

In conclusion, the mechanical properties of the tissue environment may play a significant role in regulation of initial lymphatic function. Vessels surrounded by loose, compliant tissue may serve as distensible reservoirs of drained interstitial fluid and privileged sites of lymph formation. A fast and efficient transmission of tissue forces to the vessel lumen might instead enhance lymph progression/propulsion in vessels surrounded by stiff tissue. Since muscular tissue stiffness increases during contraction, in lymphatic vessels draining the skeletal muscles, the heart or the diaphragm, lymph formation and propulsion is guaranteed, even in the absence of lymphatic smooth muscle cells, by tissue displacement. In contrast, in lymphatics running through soft compliant tissues, a well-developed layer of lymphatic smooth muscle cells is required to generate (a) transmural pressure gradients promoting lymph formation, (b) intraluminal pressure waves propelling fluid through the conduits, and (c) phasic changes of wall stiffness favouring filling of a compliant lymphangion during smooth muscle relaxations and

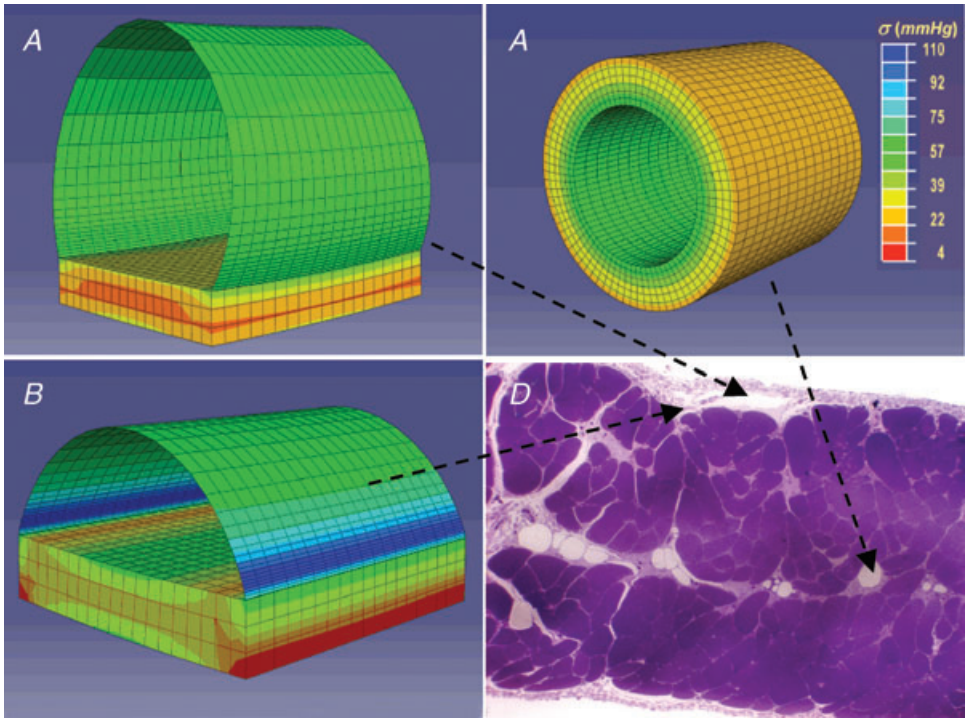

Figure 6. Three-dimensional modelling of the lymphatic vessel wall
Stress distribution maps obtained through finite element modelling of diaphragmatic initial lymphatics located as indicated on the microphotograph of the transverse section of the diaphragm, panel *D*. *A*, immediately beneath the mesothelium: the ellipsoidal *superficial* vessel is limited mostly by a thin wall of lymphatic endothelium plus pleural mesothelium and lies on a diaphragmatic muscular/tendinous support. *B*, deeper in the submesothelial tissue: this *intermediate* vessel is only partially delimited by a thin wall, most of the lateral surface being surrounded by the muscular/tendinous tissue. *C*, among the diaphragmatic muscular/tendinous fibres surrounded by an isotropic tissue and with a *circular* cross sectional area (modified from Moriondo *et al.* 2010). The circumferential stress (σ) distribution is identified by colours on a scale from red (low stress) to blue (high stress) as indicated by the colour scale in *C*. Vessel tensile stress was higher in submesothelial superficial (*A*) and intermediate (*B*) vessels which underwent the greatest deformation. In deeper circular vessels (*C*) surrounded by stiffer tissue, wall tension was lower and homogeneously distributed over the entire surface.

lymph propulsion along a stiffer vessel during muscle contraction. Therefore, one cannot exclude that in the critically ill patient, clinical conditions such as motor weakness, neuromuscular block and/or disturbances of smooth muscle contraction related to altered metabolism of nitric oxide or other mediators, might impair the lymphatic draining function, potentially leading to cardiovascular and respiratory disturbances which, ultimately, further compromise the patient's condition. Further studies of tissue and lymphatic biomechanics, currently little investigated, could aid prevention and treatment of disturbed interstitial fluid exchange and oedema, which are common problems in acute and chronic illness.

References

Aukland K & Reed R (1993). Interstitial–lymphatic mechanisms in the control of extracellular fluid volume. *Physiol Rev* **73**, 1–78.

Benoit JN, Zawieja DC, Goodman AH & Granger HJ (1989). Characterization of intact mesenteric lymphatic pump and its responsiveness to acute edemagenic stress. *Am J Physiol Heart Circ Physiol* **257**, H2059–H2069.

Burgeson RE, Lunstrum GP, Rokosova B, Rimberg CS, Rosenbaum LM & Keene DR (1990). The structure and function of type VII collagen. *Ann N Y Acad Sci* **580**, 32–43.

Casley-Smith JR & Florey HW (1961). The structure of normal small lymphatics. *Q J Exp Physiol Cogn Med Sci* **46**, 101–106.

Castenholz A (1987). Structural and functional properties of initial lymphatics in the rat tongue: scanning electron microscopic findings. *Lymphology* **20**, 112–125.

Chen M, Marinkovich MP, Veis A, Cai X, Rao CN, O'Toole EA & Woodley DT (1997). Interactions of the amino-terminal noncollagenous (NC1) domain of type VII collagen with extracellular matrix components. A potential role in epidermal-dermal adherence in human skin. *J Biol Chem* **272**, 14516–14522.

Davis MJ, Wu X, Nurkiewicz TR, Kawasaki J, Davis GE, Hill MA & Meininger GA (2001). Integrins and mechanotransduction of the vascular myogenic response. *Am J Physiol Heart Circ Physiol* **280**, H1427–H1433.

Galie P & Spilker RL (2009). A two-dimensional computational model of lymph transport across primary lymphatic valves. *J Biomech Eng* **131**, 111004.

Granger H, Laine G, Barnes G & Lewis R (1984). Dynamics and control of transmicrovascular fluid exchange. In *Edema*, ed. Staub N & Taylor A, pp. 189–228. Raven Press, New York.

Grimaldi A, Moriondo A, Sciacca L, Guidali ML, Tettamanti G & Negrini D (2006). Functional arrangement of rat diaphragmatic initial lymphatic network. *Am J Physiol Heart Circ Physiol* **291**, H876–H885.

Hargens AR & Zweifach BW (1977). Contractile stimuli in collecting lymph vessels. *Am J Physiol Heart Circ Physiol* **233**, H57–H65.

Hocking DC, Titus PA, Sumagin R & Sarelius IH (2008). Extracellular matrix fibronectin mechanically couples skeletal muscle contraction with local vasodilation. *Circ Res* **102**, 372–379.

Keene DR, Sakai LY, Lunstrum GP, Morris NP & Burgeson RE (1987). Type VII collagen forms an extended network of anchoring fibrils. *J Cell Biol* **104**, 611–621.

Leak LV (1970). Electron microscopic observations on lymphatic capillaries and the structural components of the connective tissue–lymph interface. *Microvasc Res* **2**, 361–391.

McHale N & Roddie I (1976). The effect of transmural pressure on pumping activity in isolated bovine mesentheric lymphatic vessels. *J Physiol* **261**, 255–269.

Mawhinney HJ & Roddie IC (1973). Spontaneous activity in isolated bovine mesenteric lymphatics. *J Physiol* **229**, 339–348.

Miserocchi G, Mariani E & Negrini D (1982). Role of the diaphragm in setting liquid pressure in serous cavities. *Respir Physiol* **50**, 381–392.

Miserocchi G, Negrini D, Mukenge S, Turconi P & Del Fabbro M (1989). Liquid drainage through the peritoneal diaphragmatic surface. *J Appl Physiol* **66**, 1579–1585.

Moriondo A, Boschetti F, Bianchin F, Lattanzio S, Marcozzi C & Negrini D (2010). Tissue contribution to the mechanical features of diaphragmatic initial lymphatics. *J Physiol* **588**, 3957–3969.

Moriondo A, Mukenge S & Negrini D (2005). Transmural pressure in rat initial subpleural lymphatics during spontaneous or mechanical ventilation. *Am J Physiol Heart Circ Physiol* **289**, H263–H269.

Negrini D & Del Fabbro M (1999). Subatmospheric pressure in the rabbit pleural lymphatic network. *J Physiol* **520**, 761–769.

Negrini D, Del Fabbro M, Gonano C, Mukenge S & Miserocchi G (1992). Distribution of diaphragmatic lymphatic lacunae. *J Appl Physiol* **72**, 1166–1172.

Negrini D, Moriondo A & Mukenge S (2004). Transmural pressure during cardiogenic pressure oscillations in rodent diaphragmatic lymphatic vessels. *Lymphat Res Biol* **2**, 69–81.

Negrini D, Mukenge S, Del Fabbro M, Gonano C & Miserocchi G (1991). Distribution of diaphragmatic lymphatic stomata. *J Appl Physiol* **70**, 1544–1549.

Ohhashi T, Azuma T & Sakaguchi M (1980). Active and passive mechanical characteristics of bovine mesenteric lymphatics. *Am J Physiol Heart Circ Physiol* **239**, H88–H95.

Reddy NP & Staub NC (1981). Intrinsic propulsive activity of thoracic duct perfused in anesthetized dogs. *Microvasc Res* **21**, 183–192.

Rousselle P, Keene DR, Ruggiero F, Champliaud MF, Rest M & Burgeson RE (1997). Laminin 5 binds the NC-1 domain of type VII collagen. *J Cell Biol* **138**, 719–728.

Rutkowski JM, Markhus CE, Gyenge CC, Alitalo K, Wiig H & Swartz MA (2010). Dermal collagen and lipid deposition correlate with tissue swelling and hydraulic conductivity in murine primary lymphedema. *Am J Pathol* **176**, 1122–1129.

Sakai LY, Keene DR, Morris NP & Burgeson RE (1986). Type VII collagen is a major structural component of anchoring fibrils. *J Cell Biol* **103**, 1577–1586.

Scallan JP & Huxley VH (2010). *In vivo* determination of collecting lymphatic vessel permeability to albumin: a role for lymphatics in exchange. *J Physiol* **588**, 243–254.

Schmid-Schöenbein G (1990). Microlymphatics and lymph flow. *Physiol Rev* **70**, 987–1019.

Stratman AN, Saunders WB, Sacharidou A, Koh W, Fisher KE, Zawieja DC, Davis MJ & Davis GE (2009). Endothelial cell lumen and vascular guidance tunnel formation requires MT1-MMP-dependent proteolysis in 3-dimensional collagen matrices. *Blood* **114**, 237–247.

Sun Z, Martinez-Lemus LA, Hill MA & Meininger GA (2008). Extracellular matrix-specific focal adhesions in vascular smooth muscle produce mechanically active adhesion sites. *Am J Physiol Cell Physiol* **295**, C268–C278.

Takada M (1971). The ultrastructure of lymphatic valves in rabbits and mice. *Am J Anat* **132**, 207–217.

Trzewik J, Mallipatty S, Artmann G, Delano F & Schmid-Schöenbein G (2001). Evidence for a second valve system in lymphatic endothelial microvalves. *FASEB J* **15**, 1711–1717.

Tsilibary EC & Wissig SL (1983). Lymphatic absorption from the peritoneal cavity: regulation of patency of mesothelial stomata. *Microvasc Res* **25**, 22–39.

Wang N (1998). Antomy of the pleura. *Clin Chest Med* **19**, 229–240.

Wang NS (1975). The preformed stomata connecting the pleural cavity and the lymphatics in the parietal pleura. *Am Rev Resp Dis* **111**, 12–20.

Zhang RZ, Gashev AA, Zawieja DC & Davis MJ (2007). Length–tension relationships of small arteries, veins, and lymphatics from the rat mesenteric microcirculation. *Am J Physiol Heart Circ Physiol* **292**, H1943–H1952.

Zweifach BW & Prather JW (1975). Micromanipulation of pressure in terminal lymphatics in the mesentery. *Am J Physiol* **228**, 1326–1335.